Lactate transporters in the rat barrel cortex sustain whisker-dependent BOLD fMRI signal and behavioral performance

Hélène Roumes, Charlotte Jollé, Jordy Blanc, Imad Benkhaled, Carolina Piletti Chatain, Philippe Massot, Gérard Raffard, Véronique Bouchaud, Marc Biran, Catherine Pythoud, et al.

Lactate shuttling in the rat barrel cortex sustains whisker-dependent BOLD fMRI signal and behavioral performance

Hélène Roumes[1,#], Charlotte Jollé[2,#], Jordy Blanc[1], Imad Benkhaled[1], Carolina Chatain[3], Philippe Massot[1], Leslie Mazuel[1], Gérard Raffard[1], Véronique Bouchaud[1], Marc Biran[1], Catherine Pythoud[4], Nicole Déglon[4], Eduardo Zimmer[3], Luc Pellerin[2,5,#] and Anne-Karine Bouzier-Sore[1,#,*].

[1] Univ. Bordeaux, CNRS, CRMSB, UMR 5536, F-33000 Bordeaux, France
[2] Department of Physiology, Univ. Lausanne, Lausanne, Switzerland
[3] Department of Pharmacology, Graduate Program in Biological Sciences: Biochemistry (PPGBioq) and Pharmacology and Therapeutics (PPGFT), Universidade Federal do Rio Grande do Sul, Porto Alegre, Brazil
[4] Laboratory of Cellular and Molecular Neurotherapies (LCMN), Neuroscience Research Center (CRN), Department of Clinical Neurosciences (DNC), Lausanne University Hospital, Univ. Lausanne, Lausanne, Switzerland
[5] IRTOMIT, U1082, Univ. Poitiers, F-86021 Poitiers, France
[#]Same contribution

* Anne-Karine Bouzier-Sore Univ. Bordeaux, CNRS, CRMSB, UMR 5536, F-33000 Bordeaux, France. Tel : +33 (0) 5 47 30 44 24. Fax : +33 (0) 5 57 57 45 56. E-mail : akb@rmsb.u-bordeaux.fr
https://orcid.org/0000-0002-3470-0940

DOI Number : 10.1073/pnas.2112466118

Classification
Biological Sciences, Neurosciences.

Keywords
Brain metabolism, Monocarboxylate transporter, fMRI, MRS, Learning, Memory.

Author Contributions
AKBS has conceived and designed the project, acquired and analyzed fMRI, *in vivo* and *ex vivo* MRS data and wrote the article. HR has acquired and analyzed MRI and NMR data, has performed rescue experiments and has contributed to the writing of this article. IB has performed BOLD fMRI quantifications. CJ has produced the MCT-KD animal, has set up and performed the behavioral studies and has contributed to the writing of this article. JB has acquired and analyzed MRI and NMR data, and has contributed to the rescue experiments. GR and PM have conceived the whisker activation MRI-compatible system. LM has set up the *in vivo* MRS protocol. MB has acquired *ex vivo* MRS data. VB has prepared the perchloric acid extracts. ND and CP have designed and produced the AAV vectors. CC and EZ have contributed to the writing of this article. LP has contributed to the conception and design of the project, to data analyses and to the writing of this article.

Abstract

Lactate is an efficient neuronal energy source even in presence of glucose. However, the importance of lactate shuttling between astrocytes and neurons for brain activation and function remains to be established. For this purpose, metabolic and hemodynamic responses to sensory stimulation have been measured by fMRS and BOLD fMRI after downregulation of either neuronal MCT2 or astroglial MCT4 in the rat barrel cortex. Results show that the lactate rise in the barrel cortex upon whisker stimulation is abolished when either transporter is downregulated. Under the same paradigm, the BOLD response is prevented in all MCT2-downregulated rats while only about half of the MCT4-downregulated rats exhibited a loss of the BOLD response. Interestingly, MCT4-downregulated animals showing no BOLD response were rescued by peripheral lactate infusion while this treatment had no effect on MCT2-downregulated rats. When animals were tested in a novel object recognition task, MCT2-downregulated animals were impaired in the textured but not in the visual version of the task. For MCT4-downregulated animals, while all animal succeeded in the visual task, a similar segregation in two groups as observed for BOLD experiments was evidenced with half of the animals exhibiting a deficit in the textured task. Our data demonstrate that lactate shuttling between astrocytes and neurons is essential to give rise to both neurometabolic and neurovascular couplings, which form the basis for the detection of brain activation by functional brain imaging techniques. Moreover, our results establish that this metabolic cooperation is required to sustain behavioral performance based on cortical activation.

Significance Statement

For decades, it was claimed that glucose was the sole and sufficient energy substrate to sustain neuronal activity and brain function. Our results challenge this view by demonstrating that despite glucose availability, lactate shuttling from astrocytes to neurons *via* monocarboxylate transporters is necessary to give rise to the BOLD signal (used as a surrogate marker for neuronal activation) in the rat cerebral cortex following whisker stimulation. Moreover, lactate shuttling turned out to be also essential for sustaining behavioral performance associated with activation of the rat barrel cortex. These findings call for a reappraisal of neuroenergetics and its role in determining brain function.

Introduction

In the past 25 years, a major revolution in the field of brain energy metabolism has occurred. While it was believed classically that glucose is the sole valuable energy substrate for neurons, it is now admitted that under certain circumstances, alternative substrates can serve as fuels and replace glucose, at least partially, even in the adult brain. This is the case for lactate. Indeed, it was shown that lactate provided from the periphery through the blood circulation is efficiently used by the brain in animals (1) and humans (2-4). In addition to peripheral supply, the brain itself has the capacity to internally produce lactate from peripheral glucose. This process of activity-dependent lactate transfer is named ANLS (5) and has received a large support in the literature based on *in vitro* (6, 7), *ex vivo* (1) and *in vivo* experiments (8). It was also shown that lactate supply by glial cells to neurons is a fundamental process that has been conserved during evolution as it was found to be present in invertebrates as well (e.g. flies) (9, 10). Nevertheless, some recent studies have provided evidence that direct glucose utilization by neurons also takes place during activation (11), (12) and seems essential at least for some aspects of neuronal activity (13), (14). These observations call for further *in vivo* investigations to assess the contribution of these energy supply modes to sustain brain activities ranging from metabolic and hemodynamic responses associated with brain activation to behavioral performances.

It has been well documented that activation of a brain region (e.g. hippocampus or cortex) leads to a transient increase in lactate concentration within the activated area in rodents (15-17) and in humans (18, 19). Such an observation might reflect a transient mismatch between lactate production and utilization/disposal by brain cells but the exact origin is unknown. The capacity to release or utilize lactate is determined by the expression of specific transporters named monocarboxylate transporters (MCT). Three members of this family have been identified in the central nervous system (20). MCT2 is the predominant neuronal lactate transporter (21). MCT4 expression is prominent on astrocytes (22) while MCT1 expression is more ubiquitous with strong expression on endothelial cells of blood vessels as well as on glial cells (23). Previously, it was shown that reducing MCT2 expression (which allows neuronal lactate uptake) interfered with blood oxygen level-dependent (BOLD) fMRI signal, which depends on local, activity-dependent change in blood flow and is used as a surrogate marker for neuronal activity to perform functional brain imaging (17). Recently, new viral vector tools have been developed that allow the downregulation of either MCT2 or MCT4 expression in a cell-specific manner *in vivo* (24). In the present study, we took advantage of this approach to determine the importance of both transporters and by extension, of lactate shuttling between astrocytes and neurons, in both metabolic and hemodynamic

responses as well as in behavioral performances associated with activation of the whisker-to-barrel system in rats.

Results

Cortical lactate accumulation caused by whisker stimulation is prevented by either neuronal MCT2 or astroglial MCT4 downregulation

The impact of downregulating either the neuronal MCT2 or the astroglial MCT4 transporter in the rat barrel cortex on a metabolic response to whisker stimulation was evaluated by functional MRS (fMRS) *in vivo*. Whiskers were stimulated directly into the magnet, using a MRI-compatible air-puff system. The paradigm was composed of a succession of a 20 sec activation period (8 Hz) followed by a 10 sec rest to avoid neuronal desensitization (**Figure 1A**)**.** *In vivo* ^{1}H-MRS was acquired in a 2x2.5x3 mm-voxel located in the left barrel cortex (**Figure 1B**). A first acquisition was performed at rest (**Figure 1B**, blue spectra). Then right whiskers were stimulated and a second acquisition was recorded (**Figure 1B**, red spectra). Functional MRS was performed in rats treated with a control adeno-associated vector (AAV) expressing a non-specific sequence (Ctr; white), or rats injected with vectors inducing the knockdown MCT2 (MCT2-KD; purple) and MCT4-KD (orange). The signal from protons of the methyl group of lactate is located at 1.32 ppm. The subtraction of the two spectra (activated – rest) is represented in black. While an increase in lactate content in the barrel cortex can be observed in Ctr rats, this increase was abolished both in MCT2- and MCT4-KD rats. Quantification of metabolite contents was performed using LCModel and the ratio [lactate content during whisker activation] over [lactate content at rest] is presented in **Figure 1C**. This ratio was 1.25 ± 0.05 in control rats, indicating a 25% increase in lactate content during whisker activation, while this ratio was 1.03 ± 0.04 and 1.04 ± 0.04, in MCT2- and MCT4-KD rats, respectively, which confirms the absence of lactate increase in these animals. No statistical difference was found between Ctr (1.25 ± 0.05, n=23) and uninjected rats (1.30 ± 0.09, n=18).

To determine the origin of the lactate that accumulates during whisker activation, [1-^{13}C]glucose was infused in awake rats. During the 1h-infusion, right whiskers were stimulated (same paradigm as the one used for *in vivo* MRS, **Figure 2A**). At the end of the infusion, both right (at rest) and left (activated) barrel cortices were removed (**Figure 2A**) and *ex vivo* MRS was performed on the perchloric acid extracts using a proton-observed carbon-edited sequence. This sequence allowed to calculate some metabolite specific enrichments, which represents the percentage of ^{13}C that was incorporated into a carbon position from the ^{13}C-labeled substrate that was infused (**Supplementary Table 1**). For Ctr rats, results indicate an increase in the specific enrichment of lactate carbon 3 (C3) between rest and activated barrel cortices, while the one of glutamine C4 decreased. For both MCT2- and MCT4-KD rats, no statistical difference between rest and activated barrel cortices was found. Comparison of lactate C3 specific enrichments between the right barrel cortex (resting hemisphere) and the left one (activated hemisphere) for each individual rat is shown in **Figure 2B** (Ctr)**, C** (MCT2) and **D** (MCT4). For Ctr rats, it can be clearly seen that whisker stimulation led to an increase in the incorporation of ^{13}C in lactate, indicating that more [3-^{13}C]lactate was produced from the infused precursor, [1-^{13}C]glucose, in the activated brain area. This was not observed for MCT2-KD rats. Concerning MCT4-KD rats, two animals showed a clear increase in the specific enrichment of lactate C3 between the right and the left hemispheres, whereas an obvious decrease was measured in 3 animals and slightly the same values were observed in 7 MCT4-KD rats. Quantification is presented **Figure 2E** and indicates that lactate C3 specific enrichment increased between resting and activated barrel cortices only in Ctr rats (+30%).

Cortical BOLD signal triggered by whisker activation requires MCT2-dependent neuronal lactate shuttling provided at least in part by astrocytes via MCT4

To understand why no metabolic response (observed as lactate accumulation) was detected in the barrel cortex during whisker stimulation in MCT2- and MCT4-KD rats, BOLD fMRI was performed. The 5-min paradigm used during whisker stimulation was the same as the one used during *in vivo* MRS and is presented **Figure 3A**. For Ctr rats, a positive BOLD signal was recorded in 95% of the rats (**Figure 3B**, n = 22). When the neuronal monocarboxylate transporter (MCT2) was downregulated, a positive BOLD fMRI signal was observed in only 12% of the animals. Moreover, in the 4 BOLD-positive MCT2-KD rats, brain activation level was much lower as shown in **Figure 3C** (only signals in BOLD responding animals were quantified). In the MCT4-KD group, 53% of the animals had a positive BOLD signal. For these MCT4-BOLD responding animals, no statistical difference was found in BOLD signal intensity

compared to Ctr rats. However, nearly half of the MCT4-KD rats had no BOLD fMRI signals (8/17 animals).

Rescue experiments were performed in Ctr, MCT2-KD and MCT4-KD rats (**Figure 3D**). For these experiments, a first BOLD fMRI was acquired, then lactate was infused *via* the tail vein to the animal, and a second BOLD fMRI was recorded,10min after starting lactate infusion (this time point was determined such as the lactate concentration in the barrel cortex, measured by *in vivo* MRS, was the highest, **Supplementary Figure 1**). When sodium lactate was infused during whisker activation, no difference was observed in BOLD fMRI signals measured before or during lactate infusion, neither in Ctr rats (positive BOLD fMRI signal before or during lactate infusion), nor in MCT2-KD rats (no BOLD signal, before or during lactate infusion). Interestingly, data for MCT4-KD animals can be clearly divided into two sub-groups; responding animals (during the first BOLD fMRI experiment, called MCT4 Resp) and non-responding animals (MCT4 Non resp). Indeed, an increase in the BOLD fMRI signal was observed between the first (without lactate infusion) and the second (during lactate infusion) BOLD fMRI acquisitions in 5/9 animals. Increases in signal between the first and the second BOLD fMRI acquisitions are shown in **Figure 3E**.

Learning involving the whisker-to-barrel system requires intact neuronal MCT2 expression and at least in part intact astroglial MCT4 expression in the barrel cortex

To determine if the absence of the BOLD signal in the barrel cortex upon whisker activation can lead to a loss of function, we developed a textured novel object recognition (tNOR) task to specifically probe a barrel cortex-dependent behavior. This task was designed to test the impact of MCT knockdowns in the barrel cortex on behavioral performance and was based on two already published protocols (25, 26). Some modifications were set up to avoid any texture recognition with the forepaws and to differentiate whisker-dependent sensory experience from whisker-independent experience (the protocol is presented **Figure 4A** and objects are presented **Figure 4B**, left panel). As control, we used a classical visual novel object recognition task (vNOR; objects are presented **Figure 4B**, right panel). The absence of preference for one of the objects used was first evaluated and results indicated no preference for one of the objects for both vNOR and tNOR tasks (data not shown). The sensitivity and specificity of the test was also controlled using an N-methyl-D-aspartate (NMDA) injection in the barrel cortex to produce a localized excitotoxic lesion (27) and thus interfere with behavioral performance related to texture but not to visual information processing (**Supplementary Figure 2**). To analyze the impact of neuronal MCT2 downregulation in the S1BF area, animals were submitted to this tNOR protocol (**Figure 4C**). Unlike Ctr rats, MCT2-KD animals were unable to discriminate between the two textures in the tNOR task, reflecting a dysfunction of the barrel cortex. Indeed, this impaired processing of somatosensory information prevented them to learn the task. However, in the vNOR task, their learning capacity was intact as they performed like Ctr rats. Because of the striking visual difference between the two objects, an additional processing of somatosensory information (*via* whisking activity) was not necessary for recognition of the objects. Thus, the vNOR task can be considered to be barrel cortex-independent, relying most likely on primarily visual information processing. The impact of downregulating the astrocytic lactate transporter MCT4 was also explored using the tNOR task (**Figure 4D**). Ctr and MCT4-KD rats were both able to discriminate the objects during the vNOR task while Ctr rats also succeeded in the tNOR task. In contrast, two distinct behaviors were observed for MCT4-KD rats in the tNOR task. As already observed during BOLD fMRI experiments, MCT4-KD rats can be divided into two sub-groups; a first sub-group, that was clearly able to discriminate the textured objects while the second sub-group was unable (**Figure 4E**). Distribution of MCT4-KD animals in these two sub-groups is presented **Figure 4F**, in which half of the animals (10/18) had a discrimination index of 0.49 ± 0.04 for the tNOR and 8/18 rats had a discrimination index of 0.69 ± 0.06.

Discussion

Three decades ago, a rise in lactate levels was observed for the first time in the visual cortex of humans by *in vivo* MRS during a photic stimulation (18, 19). At that time, it was attributed to a transient increase in glycolysis over respiration during brain activation. More recently, we developed a technique to perform *in vivo* MRS during brain activation in the rat barrel cortex (28). Using this technique, our aim was to follow lactate fluctuations linked to brain activity (obtained by whisker stimulation) in animals in which key partners of the ANLS would be downregulated. Right whisker stimulation led to an increase in lactate content in the left barrel cortex (also called S1BF) in Ctr rats (receiving the viral vector but expressing a non-specific sequence). The same increase in lactate was observed in non-injected rats, indicating that the stereotactic injection of AAVs has no impact on our observed signal. Considering that the

concentration of extracellular lactate in the brain is around 1 mM, this 25-30% increase would bring lactate concentration in the S1BF area around 1.25 - 1.30 mM. Keeping in mind the huge difference between neuronal activation and *in vivo* fMRS recording scales (ms *versus* min), this new lactate concentration may reflect a new steady state, in which the lactate concentration is enhanced, putatively to support high neuronal energy needs during brain activity. This new steady state in lactate concentration in the activated S1BF during whisker stimulation can be explained either by an increase in lactate synthesis during neuronal activity, or by a decrease in its consumption. To distinguish between these two hypotheses, we performed ^{13}C-experiments in which [1-^{13}C]glucose was infused in awake animals during right whisker activation. Then, both right and left barrel cortices were analyzed by *ex vivo* ^{1}H and ^{13}C-NMR spectroscopy. We measured an increase in the specific enrichment of [3-^{13}C] lactate in the activated S1BF in Ctr rats. This means that the neuronal stimulation leads to a greater synthesis of lactate (^{13}C-labeled) in the activated zone, the precursor being [1-^{13}C]glucose infused in the blood circulation. This result confirms previous data obtained using *ex vivo* MRS on control rats (29), and indicate that lactate is produced from blood-circulating glucose within the brain area during neuronal activity, at least in the cortex.

When the neuronal lactate transporter MCT2 was downregulated in the rat barrel cortex, no lactate increase linked to whisker stimulation could be observed in this brain area. If we hypothesize that lactate is produced by astrocytes during brain activity, and is further transferred to neurons, it may be surprising not to observe an accumulation of lactate in these KD rats, in which lactate cannot enter neurons. To better understand this apparent paradox, we decided to perform BOLD fMRI experiments to detect neuronal activation (using the BOLD signal as a surrogate marker for neuronal activation). While a positive BOLD signal was observed in 95% of Ctr rats, the BOLD signal was lost in MCT2 KD rats (only a small signal was observed in 4 out of 32 animals). These results confirm previous findings obtained using a lentiviral vector to express a similar shMCT2 sequence that prevented the BOLD response in the barrel cortex upon whisker stimulation (17). Based on these data, we can conclude that downregulation of the neuronal lactate transporter leads to the suppression of the mechanism which is at the origin of the BOLD signal, and therefore to an impairment of the neurovascular coupling. Since no increase in lactate levels was measured in fMRS experiments, MCT2 downregulation also leads to an apparent impairment of the neurometabolic coupling. Thus, it can be suggested that neuronal MCT2 downregulation alters neuronal activation and its consequences (as reflected by the absence of neurovascular and neurometabolic responses) within the barrel cortex.

Similarly to MCT2, downregulation of the astroglial lactate transporter MCT4 in the rat barrel cortex prevented the lactate increase caused by whisker stimulation. In this regard, it seems that the neurometabolic coupling is impaired as well with astroglial MCT4 downregulation, emphasizing the importance of an intact lactate shuttling between astrocytes and neurons for this process. Surprisingly, for the BOLD signal, results obtained with MCT4 KD rats represent a dichotomous situation between those for Ctr rats and the ones for MCT2 KD rats. Indeed, the BOLD signal was present in about half of the animals but absent in the other half, which suggests that local brain activation (and the associated neurovascular coupling) was not systematically lost (efficiency of MCT4 downregulation after stereotaxic injection in the S1BF was previously confirmed (24)). This situation suggests the existence of a threshold-like effect. Unlike neurons, which only have the MCT2 isoform, astrocytes express both isoforms 1 and 4. We can then assume that for MCT4 KD rats, the presence of MCT1 transporters still allows some lactate release. This export would be insufficient to measure by fMRS the same steady state level as the one measured in Ctr rats upon activation, but would be sufficient, at least in some rats, to maintain the appearance of the BOLD signal in the activated zone. Indeed, if enough lactate comes out of the astrocyte, or is sufficiently present in the extracellular space, it can then be sensed by neurons (MCT2 is still present). If used extensively, such as during brain activation, then lactate cannot accumulate in the extracellular space and no increase can be measured during *in vivo* fMRS. According to this hypothesis, astrocytes would therefore supply under physiological conditions more lactate than is necessary for neurons, which is in accordance with the new steady state level of lactate concentration that is measured. We may hypothesize that a lactate concentration threshold may exist to support brain activation, which was reached only in half of the MCT4 KD rats. This hypothesis would also fit with rescue experiments, in which lactate infusion was able to rescue the BOLD signal in non-responding MCT4 animals.

Altogether, our data suggest that lactate supply to neurons by astrocytes could somehow regulate neuronal network activity and define a new threshold of excitability. This effect would be entirely prevented by neuronal MCT2 downregulation but not systematically following astroglial MCT4

downregulation, depending of the resulting lactate levels which may fluctuate (depending on the extent of astroglial MCT4 downregulation). Indeed, it was recently shown that lactate acts as a signal to regulate neuronal excitability (30). This action of lactate is mediated by ATP-sensitive potassium channels which are expressed by all types of cortical neurons, including subtypes of glutamatergic neurons. It is purported that such an effect of lactate over an area corresponding to a barrel within the S1BF area would promote the capacity of the neuronal network within that structure to fine tune in a coordinated manner neuronal processing and promote learning and memory processes.

The possibility that reducing neuronal MCT2 expression or astroglial MCT4 expression might also interfere with behavioral performance that relies on the activation of the barrel cortex was tested. MCT2 downregulation led to an important deficit of S1BF function, reflected by the absence of discrimination between the objects during the tNOR task. However, those animals were still able to discriminate the objects during the vNOR task. Results obtained in astroglial MCT4 downregulated animals reflected those obtained in BOLD fMRI. About half of the animals were impaired in the tNOR task. These results show that the memory deficit seen in the tNOR task was caused by a specific deficit in the processing of somatosensory information in the barrel cortex, and not a global impairment in learning or a deficit related to the other brain structures involved in the task. These findings concur with several others indicating that interfering with MCT expression on astrocytes and neurons, and/or lactate shuttling between the two cell types, alters learning and memory performances in a number of spatial and non-spatial tasks (31-36). While previous studies were targeting either the hippocampus or the striatum, our study is demonstrating for the first time an effect on behavioral performance after modifying expression in a specific cortical area. This finding reinforces the view that lactate shuttling between astrocytes and neurons is a fundamental process present in various brain regions that is essential to sustain cognition.

In conclusion, our data indicate that lactate shuttling *via* MCTs between astrocytes and neurons is not only necessary to give rise to the neuro-vascular and the neuro-metabolic coupling linked to brain activity, but also to support cognitive function subserved by this local brain activation.

Materials and Methods

1. Animals

All animal procedures were conducted in accordance with the Animal Experimentation Guidelines of the European Communities Council Directive of November 24, 1986 (86/609/EEC). Protocols met the ethical guidelines of the French Ministry of Agriculture and Forests, and were approved by the local ethics committees (Comité d'éthique pour l'expérimentation Animale Bordeaux n°50112090-A and the Swiss “Service de la Consommation et des Affaires Vétérinaires, SCAV, authorization n°3101.1). Male Wistar RJ-HAN (Janvier Laboratories, France) were kept on a 12:12 hours light:dark cycle with food and water *ad libitum*.

2. AAV2/DJ-based viral vector generation

AAV2/DJ-based viral vectors were prepared exactly as described in detail in Jollé *et al.* (45). Briefly, four constructs were made to target alternatively neurons or astrocytes. For neuron-specific expression, a shRNA sequence targeting MCT2 (shMCT2; TAGGATTAATAGCCAACACTA) or a control non-coding sequence (shUNIV2; TGTATCGATCACGAGACTAGC) embedded in a miR30E sequence was positioned after a mCherry sequence under the control of a CBA (Chicken-β-actin) promoter. For astrocyte-specific expression, a shRNA sequence targeting MCT4 (shMCT4; GGTGAGCTATGCTAAGGATAT) or a control non-coding sequence (shUNIV4; TGTATCGATCACGAGACTAGC) embedded in a miR30E sequence was positioned after a mCherry sequence under the control of a G1B3 (a Glial Fibrillary Acidic Protein derived) promoter (37). Each construct was incorporated in an AAV2/DJ serotype to obtain four distinct AVV2/DJ-based viral vectors. All these viral vectors had been tested previously for their specificity and efficacy in the rat barrel cortex (45). Since no difference was observed between animals injected with either AAV2/DJ-CBA-shUNIV2 or AAV2/DJ-G1B3-shUNIV4, data from these animals were pooled and considered as control (Ctr) data.

3. Stereotaxic injection

Surgeries were performed on seven-week-old animals. Animals were anesthetized with isoflurane (5% for the induction and 3% to maintain the anesthesia). AAVs or PBS were injected in one site/hemisphere (S1BF: Anteroposterior = - 2,3 mm; Mediolateral = ± 5 mm; Dorsoventral = - 3 mm). Viral vectors were injected with 34G steel cannula fixed on a cannula holder and linked to a 10 µL Hamilton syringe and an infusion pump. For each site, 4 µL of viral vector were injected at 0.2 µL/min. Cannulas were left in the brain for 5 minutes after the injection, and then slowly removed. Skin was closed using 4.0 sterile suture thread. Sterile NaCl 0.9% solution (1 mL) was delivered to the rat by intra-peritoneal injection to

avoid dehydration after surgery, and healing cream was applied on the head. Sugar-taste Paracetamol was delivered to the animal in water (1g/cage for rats) during 72h. Animals were monitored until complete awakening, and every day during three days after the surgery. All viral vectors were injected at a final concentration of $1x10^8$ vg/site.

4. *In vivo* functional ^{1}H-MRS and BOLD fMRI

Experiments were conducted on a 7T Bruker BioSpec system (70/20, Ettlingen, Germany) equipped with a 20-cm horizontal bore, a gradient system capable of 660 mT/m maximum strength and 110 µs rise time. A surface coil (10-mm inner diameter, Bruker) was used for excitation and signal reception. Rats were anaesthetized using medetomidine hydrochloride (Domitor, Vetoquinol SA, France, 1 mg/mL, 240 µg/kg/h – perfusion rate: 20 µL/min). Whisker activation was performed directly into the magnet using an air-puff system (28). For this purpose, right whiskers were taped such as a sail was made and this sail was blown at 8 Hz during the acquisition time (activation paradigm: 20s activation – 10s rest, duration 5 min). In order to place correctly the voxel in the S1BF area, a T_2-weighted sequence was performed (RARE sequence): 16 slices, 1 mm thick, FOV 5x5 cm. A voxel was then located in the S1BF area (2 x 2.5 x 3 mm) and *in vivo* spectroscopy was performed either at rest or during whisker activation using a LASER sequence (TE 20 ms, TR 2500 ms, 256 scans). Spectra were analyzed and lactate was quantified using LCModel (Provencher) software.

Finally, functional imaging was performed. The BOLD response was measured (using the activation paradigm) in four slices of 0.7 mm thickness using a single short gradient echo, echo planar imaging sequence (TR = 500ms, TE = 16.096 ms, field of view 25x25 mm², matrix size 96x96 and bandwidth of 33333 Hz). Images were reconstructed and analyzed using FUN TOOL fMRI processing (Bruker software).

5. Rescue experiments

Rats were anaesthetized using medetomidine hydrochloride (Domitor, Vetoquinol SA, France, 1 mg/mL, 240 µg/kg/h – perfusion rate: 20 µL/min) as previously, using an amagnetic tail vein catheter. A three-way stopcock was used for lactate infusion (sodium salt, 534 mM, with a flow rate monitored from 15 mL/h to 1.23 mL/h during the first 25 min). Measurement of the BOLD response was performed twice. The first acquisition was performed during whisker activation, without lactate infusion. Then, lactate infusion was initiated and the second BOLD experiment was started 10 min after the beginning of the lactate infusion. Lactate concentration was the highest in the barrel cortex in this time window, as previously determined by *in vivo* ^{1}H-MRS performed every 5 min in the barrel cortex during the lactate infusion protocol period (25 min).

6. *Ex vivo* MRS

Whisker activation on awake animals. Experiments were performed in awake animals six weeks after AAV injection. Animals were slightly held on a Plexiglas support during the stimulation. Before infusion experiments, each animal was accustomed to the experimental set up (at least 3 times, 1h) to avoid any stress and ^{13}C-infusion experiments were performed once rats demonstrated that they lie quietly. Right whiskers were mechanically stimulated at a rate of 8 Hz during 1h. To stimulate the maximum of whiskers, they were cut to an equivalent length: 2.5 cm. Infusions were performed in the tail vein during 1h (to reach the isotopic steady state), during the whisker stimulation. Rats were infused with a solution containing [1-^{13}C glucose] (750 mM, Cambridge isotope, 99% enrichment) + lactate (sodium salt, 534 mM). Intravenous infusions were carrying out using a syringe pump that allows a flux such as glucose and lactate concentrations in the blood remain constant (the infusate flow was monitored to obtain a time-decreasing exponential from 15 mL/h to 1.23 mL/h during the first 25 min after which the rate was kept unchanged). At the end of the experiment, a sample of blood was removed; rats were rapidly euthanized by cerebral-focused microwaves (5 KW, 1s, Sacron8000, Sairem), the only way to immediately stop all enzymatic activities and to avoids post-mortem artefacts such as anaerobic lactate production, as already demonstrated in (29).

S1BF areas (right -non activated- and left -activated-) were removed, using a rat brain matrix that allows precise and reproducible dissection of the selected brain regions, dipped in liquid nitrogen and kept at -80°C until NMR analyses, conducted on a Bruker DPX500 spectrometer equipped with a HRMAS (High Resolution at the Magic Angle Spinning) probe after perchloric acid extracts. Indeed, HR-MAS allows performing spectra with high spectral resolution not only directly on biopsies but also on small perchloric acid extract volumes (50 µL).

Perchloric acid extracts: A volume of 200 µL of 0.9 M perchloric acid was added to the frozen S1BF biopsies (around 30 mg) and further sonicated (at 4°C). The mixture was then centrifuged at 5000 g for 15min (4°C). The brain extract was neutralized with KOH to pH=7.2, centrifuged again to eliminate potassium perchlorate salts. Supernatant was lyophilized, the final powder was dissolved in 100 µL D_2O and bivalent cations were eliminated using Chelex™ 100 resin beads. Ethylene glycol was added and used as an external reference (1 M, peak at 63 ppm, 2 µl).

Proton-observed carbon-editing (POCE) sequence: This sequence was used to determine the ^{13}C-specific enrichment (SE) at selected metabolite carbon positions using the (^{13}C-^{1}H) heteronuclear multiquanta correlation (38, 39). Briefly, two spectra are acquired: the first scan corresponds to a standard spin-echo experiment without any ^{13}C excitation and a second scan involves a ^{13}C-inversion pulse to get coherence transfer between coupled ^{13}C and ^{1}H nuclei. Subtraction of two alternate scans leads to the editing of ^{1}H spins coupled to ^{13}C spins (scalar coupling constant JCH = 127 Hz). ^{13}C-decoupling was applied during the acquisition to collapse the ^{1}H-^{13}C coupling under a single 1H resonance. Flip angles for rectangular pulses were carefully calibrated on both radiofrequency channels before each experiment. The relaxation delay was 8s for a complete longitudinal relaxation. The ^{13}C-SE was calculated as the ratio of the area of a given resonance on the edited ^{13}C-^{1}H spectrum to its area on the standard spin-echo spectrum. The reproducibility and accuracy of the method were previously assessed using several mixtures of ^{13}C-labeled amino acids and lactate with known fractional enrichments and both were better than 5%.

7. Behavioral studies

Animals were given three weeks to recover from surgery (AAV injections). They were habituated to the housing of the behavioral area for two weeks. During the first two days of behavioral testing, rats were habituated for 10min to the circular open field arena (45 x 10 cm, light grey). The floor and walls were cleaned with ethanol 70% to avoid scent trails guiding the animals between test sessions. On the third day, the textured task of the tNOR was performed. For the first step, the animal was released on one side of the arena, facing the wall, at equal distance from the two identical objects. The objects were placed equidistant from the center of the arena and from the walls. Each rat was allowed to explore the objects for 10min. The animal was then removed from the arena for 5min. During this retention period, the arena and the objects were wiped with ethanol 70%. One of the familiar objects was replaced by the novel object. This object was visually identical to the familiar object (in size, shape, colour) but exhibited a different texture (smooth or rough). To avoid any texture discrimination coming from forepaws and to test only whisker sensitivity, only the lower part of the object had a different texture. Then for the second step, the rat was returned into the test arena and allowed to explore the objects for 10min. The time each rat spent physically exploring the objects was recorded during both steps.

On the fourth day, the visual task of the tNOR took place. The rat was allowed to explore the two identical objects for 10min. Then the rat was removed from the arena for 5min. The arena and objects were wiped with ethanol 70%. One object was replaced by a novel object. This object was visually different from the familiar one. Then the animal was reintroduced into the arena and allowed to explore the objects for 10min.

In the visual task, object A was 10 cm in diameter x 22 cm in height and object B was 10 x 10 x 20 cm. In the textured task, the two objects were 10.5 x 5 x 15.5 cm. Object A was rough and Object B was smooth.

The novelty preference index was calculated as $Preference\ Index = \frac{Time_{Object\ A/B}}{(Time_{Object\ A} + Time_{Object\ B})}$. Animals that did not explore the two objects for at least 4 seconds were excluded from the analysis. The visual and the textured tNOR tasks were recorded using Media Recorder v.4.0.2. The time of exploration was blindly and manually scored using Kinoscope v0.3.0.

8. Statistical analysis

Results are presented as mean ± SEM. Statistical analyses were performed with GraphPad Prism (v. 7.04). For behavioral analyses, a Wilcoxon's test was applied to compare the novelty preference index to 0.5 (chance value). For BOLD fMRI and fMRS, data were analyzed using ordinary one-way ANOVA followed by a Fisher's LSD test or paired-t test. Results were considered significant when $p < 0.05$.

Acknowledgments

Anne-Karine Bouzier-Sore and Luc Pellerin have received financial support from an international French (ANR)/Swiss (FNS) grant, references ANR-15-CE37-0012 and FNS n°310030E-164271. Luc Pellerin also received financial support for this project from the program IdEx Bordeaux ANR-10-IDEX-03-02. Anne-Karine Bouzier-Sore has also received financial support from the French State in the context of the "Investments for the future" Programme IdEx and the LabEx TRAIL, reference ANR-10-IDEX and ANR-10-LABX-57. Nicole Déglon has received support from the BIOS and Panacée Foundations.

References

1. A. K. Bouzier *et al.*, The metabolism of [3-(13)C]lactate in the rat brain is specific of a pyruvate carboxylase-deprived compartment. *J Neurochem* **75**, 480-486 (2000).
2. D. Smith *et al.*, Lactate: a preferred fuel for human brain metabolism in vivo. *J Cereb Blood Flow Metab* **23**, 658-664 (2003).
3. G. van Hall *et al.*, Blood lactate is an important energy source for the human brain. *J Cereb Blood Flow Metab* **29**, 1121-1129 (2009).
4. F. Boumezbeur *et al.*, The contribution of blood lactate to brain energy metabolism in humans measured by dynamic 13C nuclear magnetic resonance spectroscopy. *J Neurosci* **30**, 13983-13991 (2010).
5. L. Pellerin, P. J. Magistretti, Glutamate uptake into astrocytes stimulates aerobic glycolysis: a mechanism coupling neuronal activity to glucose utilization. *Proc Natl Acad Sci U S A* **91**, 10625-10629 (1994).
6. A. K. Bouzier-Sore *et al.*, Competition between glucose and lactate as oxidative energy substrates in both neurons and astrocytes: a comparative NMR study. *Eur J Neurosci* **24**, 1687-1694 (2006).
7. A. K. Bouzier-Sore, P. Voisin, P. Canioni, P. J. Magistretti, L. Pellerin, Lactate is a preferential oxidative energy substrate over glucose for neurons in culture. *J Cereb Blood Flow Metab* **23**, 1298-1306 (2003).
8. L. Pellerin, P. J. Magistretti, Sweet sixteen for ANLS. *J Cereb Blood Flow Metab* **32**, 1152-1166 (2012).
9. A. Volkenhoff *et al.*, Glial Glycolysis Is Essential for Neuronal Survival in Drosophila. *Cell Metab* **22**, 437-447 (2015).
10. L. Liu, K. R. MacKenzie, N. Putluri, M. Maletic-Savatic, H. J. Bellen, The Glia-Neuron Lactate Shuttle and Elevated ROS Promote Lipid Synthesis in Neurons and Lipid Droplet Accumulation in Glia via APOE/D. *Cell Metab* **26**, 719-737 e716 (2017).
11. I. Lundgaard *et al.*, Direct neuronal glucose uptake heralds activity-dependent increases in cerebral metabolism. *Nature communications* **6**, 6807 (2015).
12. C. M. Diaz-Garcia *et al.*, Neuronal Stimulation Triggers Neuronal Glycolysis and Not Lactate Uptake. *Cell Metab* **26**, 361-374 e364 (2017).
13. J. J. Laschet *et al.*, Glyceraldehyde-3-phosphate dehydrogenase is a GABAA receptor kinase linking glycolysis to neuronal inhibition. *J Neurosci* **24**, 7614-7622 (2004).
14. J. M. Ferreira, A. L. Burnett, G. A. Rameau, Activity-dependent regulation of surface glucose transporter-3. *J Neurosci* **31**, 1991-1999 (2011).
15. L. K. Fellows, M. G. Boutelle, M. Fillenz, Physiological stimulation increases nonoxidative glucose metabolism in the brain of the freely moving rat. *J Neurochem* **60**, 1258-1263. (1993).
16. Y. Hu, G. S. Wilson, A temporary local energy pool coupled to neuronal activity: fluctuations of extracellular lactate levels in rat brain monitored with rapid-response enzyme-based sensor. *J Neurochem* **69**, 1484-1490. (1997).
17. L. Mazuel *et al.*, A neuronal MCT2 knockdown in the rat somatosensory cortex reduces both the NMR lactate signal and the BOLD response during whisker stimulation. *PLoS One* **12**, e0174990 (2017).
18. J. Prichard *et al.*, Lactate rise detected by 1H NMR in human visual cortex during physiologic stimulation. *Proc Natl Acad Sci U S A* **88**, 5829-5831 (1991).
19. D. Sappey-Marinier *et al.*, Effect of photic stimulation on human visual cortex lactate and phosphates using 1H and 31P magnetic resonance spectroscopy. *J Cereb Blood Flow Metab* **12**, 584-592 (1992).
20. K. Pierre, L. Pellerin, Monocarboxylate transporters in the central nervous system: distribution, regulation and function. *J Neurochem* **94**, 1-14 (2005).
21. K. Pierre, P. J. Magistretti, L. Pellerin, MCT2 is a major neuronal monocarboxylate transporter in the adult mouse brain. *J Cereb Blood Flow Metab* **22**, 586-595 (2002).
22. K. Rosafio, X. Castillo, L. Hirt, L. Pellerin, Cell-specific modulation of monocarboxylate transporter expression contributes to the metabolic reprograming taking place following cerebral ischemia. *Neuroscience* **317**, 108-120 (2016).
23. O. Chiry *et al.*, Expression of the monocarboxylate transporter MCT1 in the adult human brain cortex. *Brain Res* **1070**, 65-70 (2006).
24. C. Jolle, N. Deglon, C. Pythoud, A. K. Bouzier-Sore, L. Pellerin, Development of Efficient AAV2/DJ-Based Viral Vectors to Selectively Downregulate the Expression of Neuronal or Astrocytic Target Proteins in the Rat Central Nervous System. *Front Mol Neurosci* **12**, 201 (2019).

25. V. Briz *et al.*, The non-coding RNA BC1 regulates experience-dependent structural plasticity and learning. *Nature communications* **8**, 293 (2017).
26. H. P. Wu, J. C. Ioffe, M. M. Iverson, J. M. Boon, R. H. Dyck, Novel, whisker-dependent texture discrimination task for mice. *Behavioural brain research* **237**, 238-242 (2013).
27. E. D. Kirby, K. Jensen, K. A. Goosens, D. Kaufer, Stereotaxic surgery for excitotoxic lesion of specific brain areas in the adult rat. *J Vis Exp* 10.3791/4079, e4079 (2012).
28. J. Blanc *et al.*, Functional Magnetic Resonance Spectroscopy at 7 T in the Rat Barrel Cortex During Whisker Activation. *J Vis Exp* 10.3791/58912 (2019).
29. D. Sampol *et al.*, Glucose and lactate metabolism in the awake and stimulated rat: a (13)C-NMR study. *Front Neuroenergetics* **5**, 5 (2013).
30. A. Karagiannis *et al.*, Lactate is a major energy substrate for cortical neurons and enhances their firing activity. *BioRxiv* 10.1101/2021.05.17.444414 (2021).
31. G. Descalzi, V. Gao, M. Q. Steinman, A. Suzuki, C. M. Alberini, Lactate from astrocytes fuels learning-induced mRNA translation in excitatory and inhibitory neurons. *Commun Biol* **2**, 247 (2019).
32. D. L. Korol, R. S. Gardner, T. Tunur, P. E. Gold, Involvement of lactate transport in two object recognition tasks that require either the hippocampus or striatum. *Behav Neurosci* **133**, 176-187 (2019).
33. C. Netzahualcoyotzi, L. Pellerin, Neuronal and astroglial monocarboxylate transporters play key but distinct roles in hippocampus-dependent learning and memory formation. *Prog Neurobiol* **194**, 101888 (2020).
34. M. Tadi, I. Allaman, S. Lengacher, G. Grenningloh, P. J. Magistretti, Learning-Induced Gene Expression in the Hippocampus Reveals a Role of Neuron -Astrocyte Metabolic Coupling in Long Term Memory. *PLoS One* **10**, e0141568 (2015).
35. L. A. Newman, D. L. Korol, P. E. Gold, Lactate produced by glycogenolysis in astrocytes regulates memory processing. *PLoS One* **6**, e28427 (2011).
36. A. Suzuki *et al.*, Astrocyte-neuron lactate transport is required for long-term memory formation. *Cell* **144**, 810-823 (2011).
37. M. Humbel *et al.*, Maximizing lentiviral vector gene transfer in the CNS. *Gene Ther* **28**, 75-88 (2021).
38. R. Freeman, T. H. Mareci, G. A. Morris, Weak satellite signals in high-resolution NMR spectra: separating the wheat from the chaff. *J Magn Reson* **42**, 341-345 (1981).
39. D. L. Rothman *et al.*, 1H-Observe/13C-decouple spectroscopic measurements of lactate and glutamate in the rat brain in vivo. *Proc Natl Acad Sci U S A* **82**, 1633-1637. (1985).

Figures and Tables

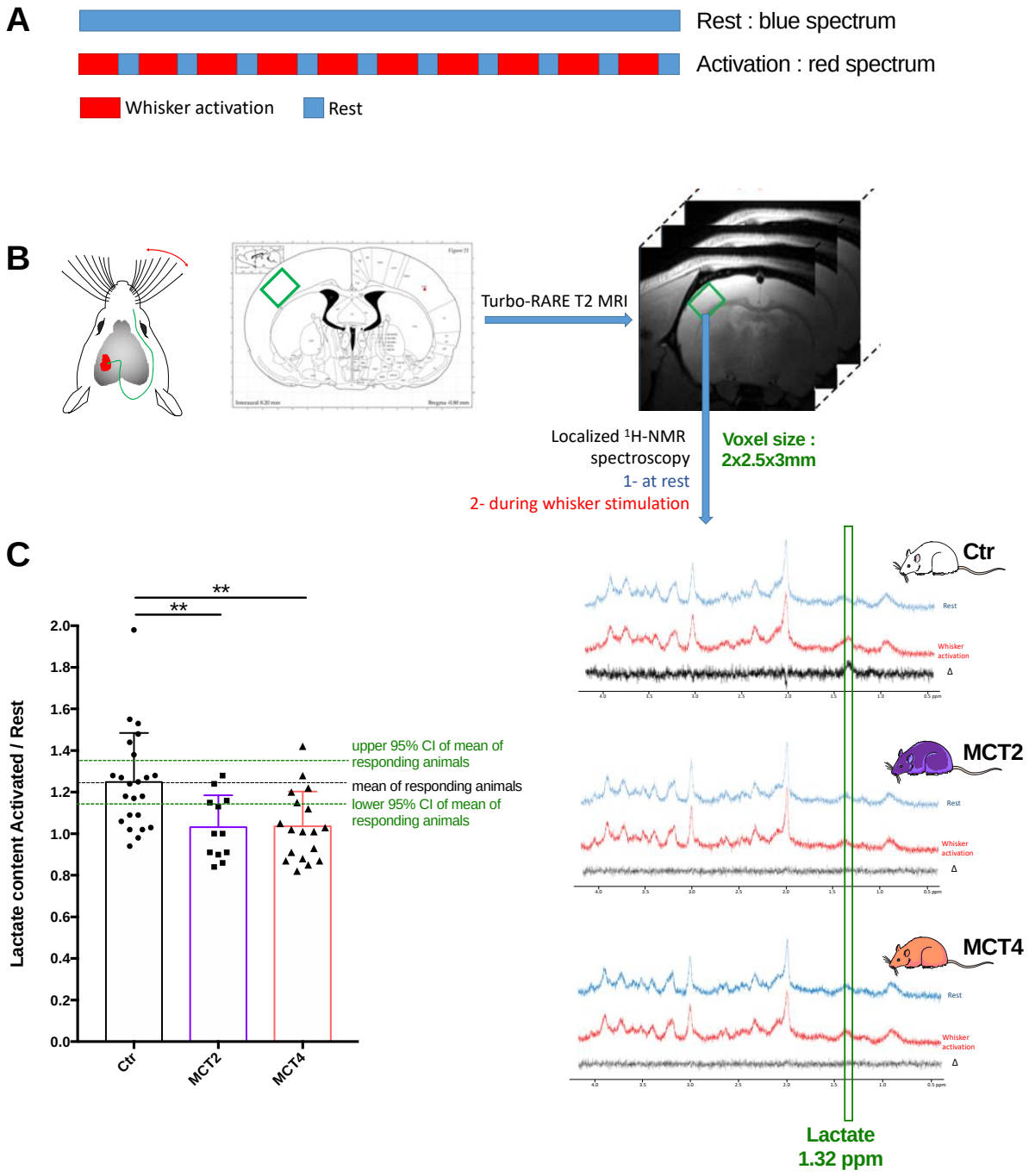

Figure 1. ***In vivo*** **functional MRS upon whisker stimulation in rats with cell-specific MCT2 or MCT4 downregulation in the barrel cortex. A:** Whisker stimulation paradigm (activation: 20sec, 8Hz; rest: 10 sec, during the entire MRS acquisition for the activation condition). **B:** The right whisker stimulation leads to the activation of the barrel cortex (also called S1BF) in the left somatosensory cortex. Voxel location for MRS is determined by comparison of T2-weighted images and rat atlas maps. Typical spectra acquired at rest (blue) and during whisker stimulation (red) for Ctr, MCT2- and MCT4-KD rats. The difference between the red and the blue spectra is shown in the black spectra. The green rectangle indicates the chemical shift of the protons from the methyl group of lactate (protons linked to lactate carbon 3) at 1.32ppm. **C:** Ratio of lactate contents during the whisker stimulation and the resting state. Ctr, n=23; MCT2, n=12; MCT4, n=18. ** p<0.004, one-way ANOVA followed by a Fisher's LSD test.

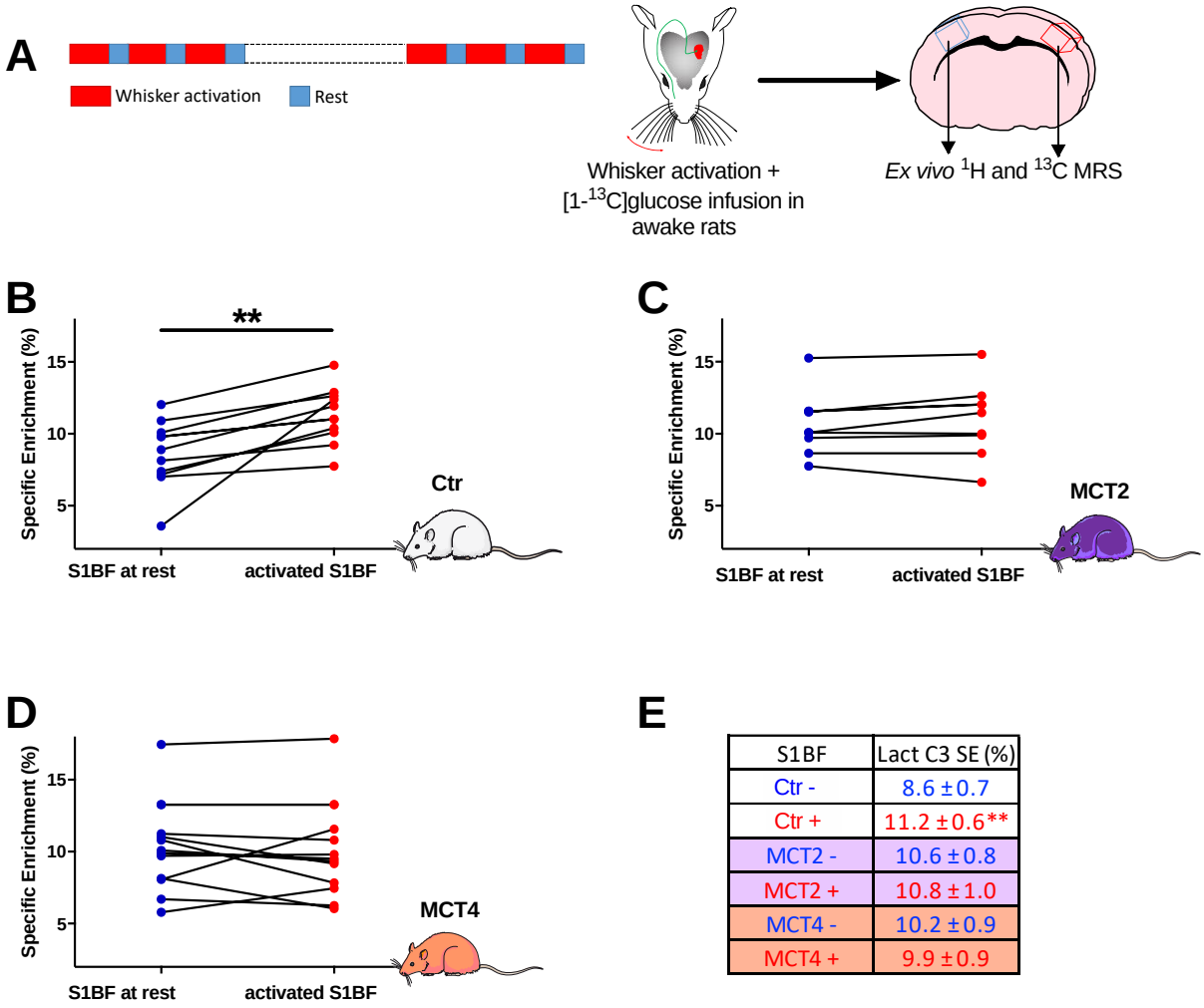

E

S1BF	Lact C3 SE (%)
Ctr -	8.6 ± 0.7
Ctr +	11.2 ± 0.6**
MCT2 -	10.6 ± 0.8
MCT2 +	10.8 ± 1.0
MCT4 -	10.2 ± 0.9
MCT4 +	9.9 ± 0.9

Figure 2. **Comparison of lactate C3 ^{13}C-specific enrichments (%) between the resting hemisphere (right S1BF, blue) and the activated hemisphere (left S1BF, red). A:** Paradigm used for whisker stimulation (activation: 20sec, 8Hz; rest: 10 sec, during the entire [1-^{13}C]glucose infusion protocol). **B:** Comparison of [3-^{13}C]lactate specific enrichment (%) for each animal between the resting and activated S1BF in Ctr rats, n=11, ** p=0.004, between right and left hemispheres, paired t-test. **C:** Comparison of [3-^{13}C]lactate specific enrichment (%) for each animal between the resting and activated S1BF in MCT2 rats, n=9. **D:** Comparison of [3-^{13}C]lactate specific enrichment (%) for each animal between the resting and activated S1BF in Ctr rats, n=13. **E:** Means values of [3-^{13}C]lactate specific enrichment (%), in the resting (Ctr-, MCT2- and MCT4-) and in the activated (Ctr+, MCT2+ and MCT4+) hemispheres, ** p=0.004, between right and left hemispheres, paired t-test.

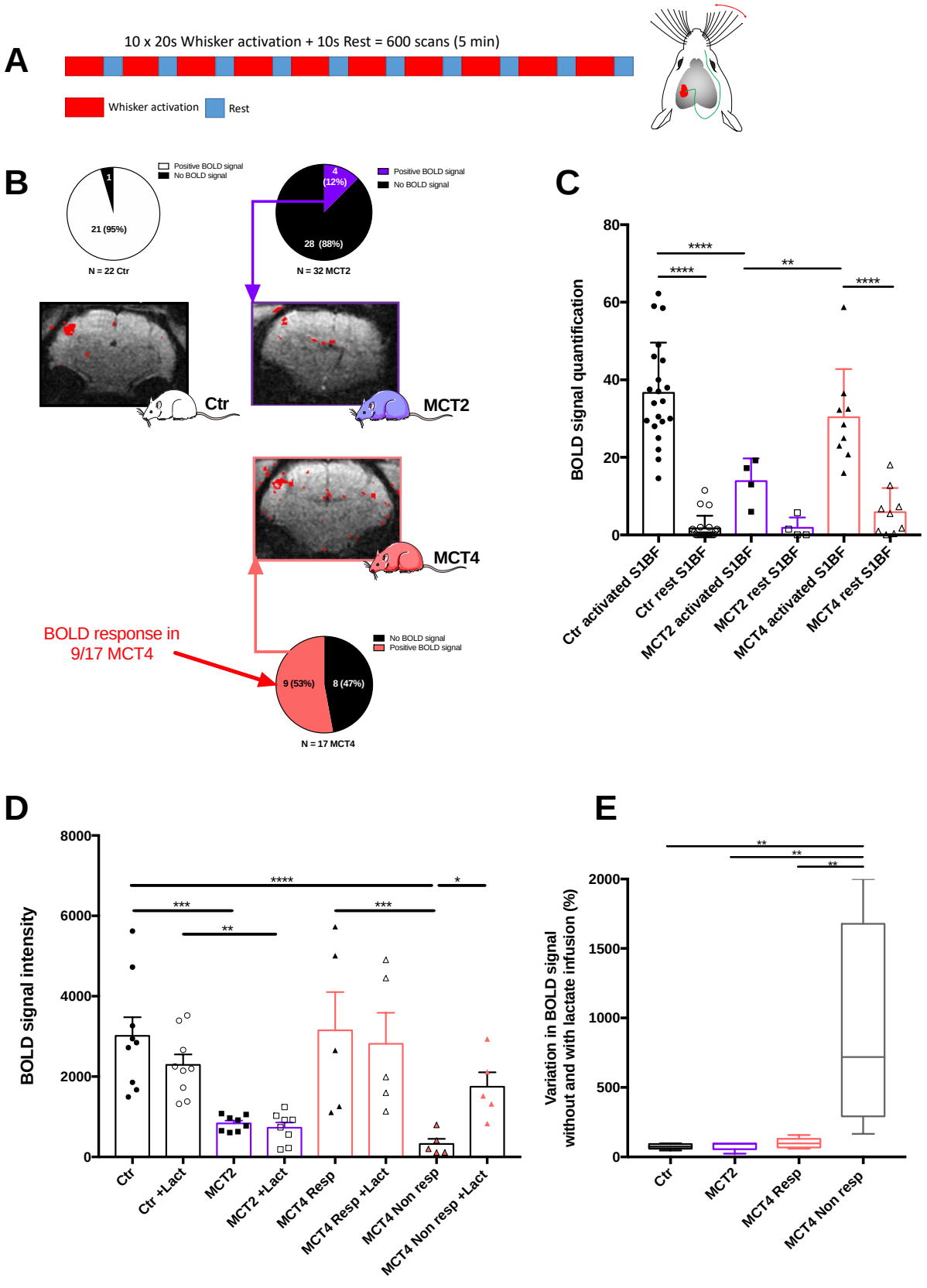

Figure 3. Effect of cell-specific MCT2 or MCT4 downregulation in the barrel cortex on the BOLD fMRI response during whisker stimulation and its putative rescue by lactate infusion. A: Description of the paradigm used for whisker stimulation. The paradigm was composed by a succession of 20 sec of activation (8 Hz) and 10 sec of rest to avoid neuronal desensitization. Total length of the paradigm was 5 min. **B:** Distribution of positive/negative responding animals and typical BOLD fMRI images for Ctr (n=22), MCT2-KD (n=32) and MCT4-KD (n=17) rats. Quantification of the BOLD fMRI

signals (only for positive-responding animals) is presented in **C**. **D:** Rescue experiments: BOLD fMRI was performed before (open symbols) and 10min after starting lactate infusion (bold symbols) in Ctr (n= 4, circles), MCT2-KD (n=4, squares) and MCT4-KD (n=9, triangles) rats. * $p<0.05$; ** $p<0.01$; *** $p<0.001$; **** $p<0.0001$; ANOVA followed by a Fisher's LSD test.

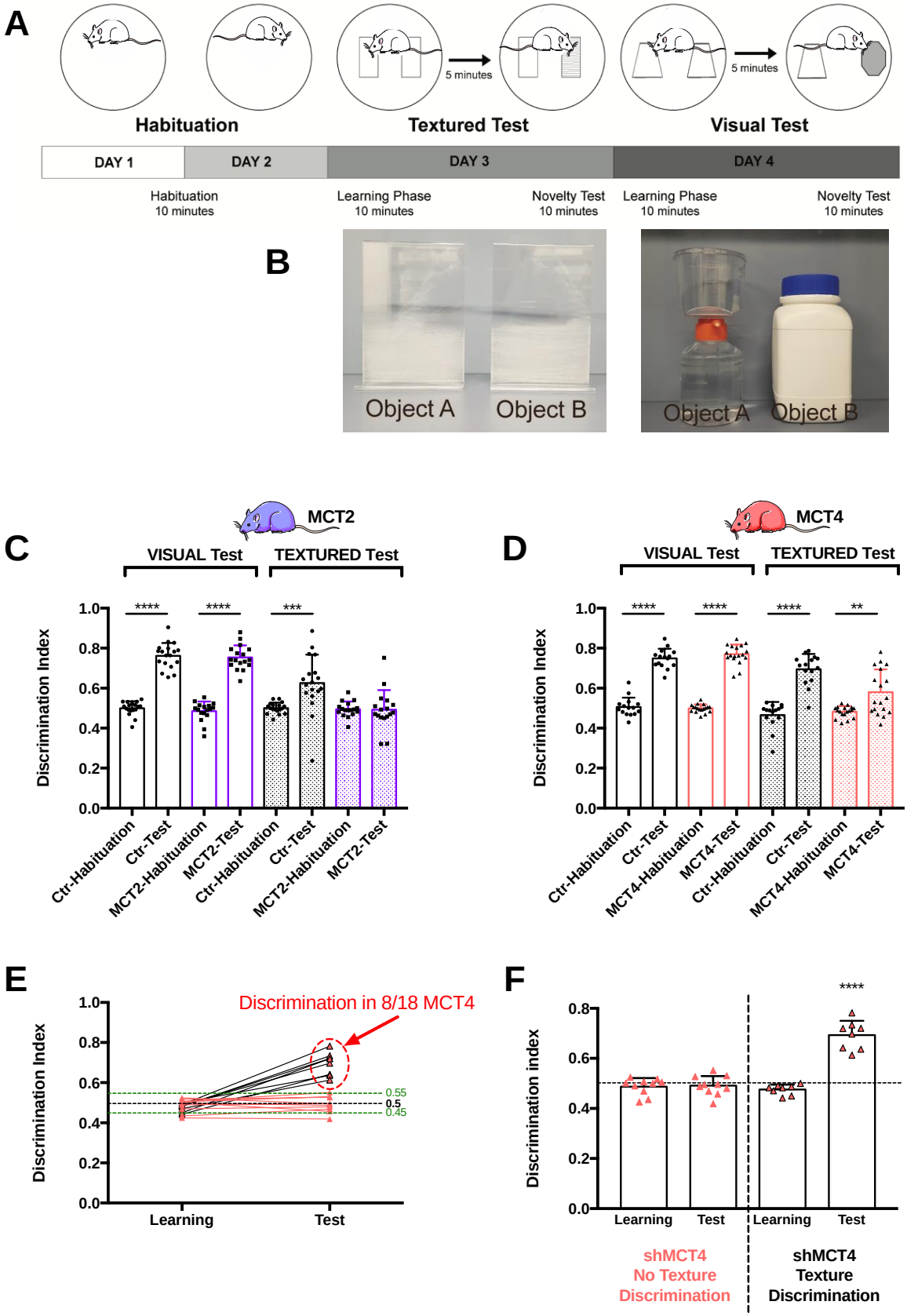

Figure 4. Effect of cell-specific MCT2 or MCT4 downregulation in the barrel cortex on performance in the visual and textured novel object recognition tasks

A: Schematic representation of the protocol to perform both the textured and visual novel recognition tasks. The test is divided in 4 consecutive days. On day 1 and 2, animals were habituated to the arena for 10 min. On the third day, the animal was submitted to the textured task, composed of 10 min of

learning, 5 min of rest and 10 min of test with one of the objects that was exchanged. In the textured task, the novel object was identical in size, shape and color but different in term of texture (smooth versus rough). Finally, on the fourth day, the animal was submitted to the visual task and for the visual task. The difference with the third day was that the novel object was different in term of shape and color. For the two last days, the time spent exploring the objects was measured. **B:** Pictures of the objects used for the textured and visual tasks. **C:** Discrimination indexes for the visual and the textured NOR for Ctr and MCT2 animals. Data are presented as mean ± SEM. *** $p<0.001$; **** $p<0.0001$. Ctr rat, n=18; MCT2 rats, n=16 rats. **D:** Discrimination indexes for the visual and the textured NOR for Ctr and MCT4 animals. Data are presented as mean ± SEM. ** $p<0.01$; **** $p<0.0001$. Ctr rat, n=15; MCT4 rats, n=18 rats. **E:** Evolution of the discrimination indexes between the learning and the test phases for MCT4 animals, n=18 rats. The black dashed line corresponds to an equal exploration of the two objects and the green dashed lines indicate the corresponding statistical limits. **F:** Discrimination indexes for the learning and the test phases for the textual NOR for the two groups of MCT4 animals defined based on **Figure 4E**. The horizontal dashed line corresponds to an equal exploration of the two objects. Orange triangles: MCT4 animals with no texture discrimination, n=10; Black and orange triangles: MCT4 animals with texture discrimination, n=8. Data are presented as mean ± SEM. **** $p<0.0001$.

Supplementary data

Supplementary Figure 1. Lactate concentration kinetics in the barrel cortex during peripheral lactate infusion. Lactate content was determined every 5 min by localized ^{1}H-NMR spectroscopy in the barrel cortex during lactate infusion (20 min) in the tail vein. In shaded grey, the selected time window to acquire the second BOLD fMRI response. n=2.

Supplementary Figure 2. Effect of an excitotoxic lesion in the barrel cortex on performance in the visual and textured novel object recognition tasks.
A: Preference indexes for the visual task of animals injected with PBS or NMDA 1M. The dashed line corresponds to chance level, when the animal equally explored the two objects. Data are presented as mean ± SEM. * p<0.05, *** p<0.001, ordinary one-way ANOVA, followed by Fisher's LSD test. n=6 rats.
B: Preference indexes for the textured task of animals injected with PBS or NMDA 1M. The dashed line corresponds to chance level, when the animal equally explored the two objects. Data are presented as mean ± SEM. * p<0.05, ordinary one-way ANOVA, followed by Fisher's LSD test. n=6.

Supplementary Table 1. ^{13}C-specific enrichment values for some metabolites (%). [1-^{13}C]glucose was infused in the tail vein and the ^{13}C incorporation in some metabolites was measured from POCE spectra of perchloric acid extracts of resting and activated S1BF in Ctr, MCT2 and MCT4 rats. Lac C3: carbon 3 of lactate; Ala C3: carbon 3 of alanine; GABA C2: carbon 2 of γ–aminobutyrate; Glu C4: carbon 4 of glutamate; Gln C4: carbon 4 of glutamine and Asp C3: carbon 3 of aspartate. * p<0.05, ordinary one-way ANOVA, followed by Fisher's LSD test. Ctr, n=11; MCT2, n=9 and MCT4, n=13.

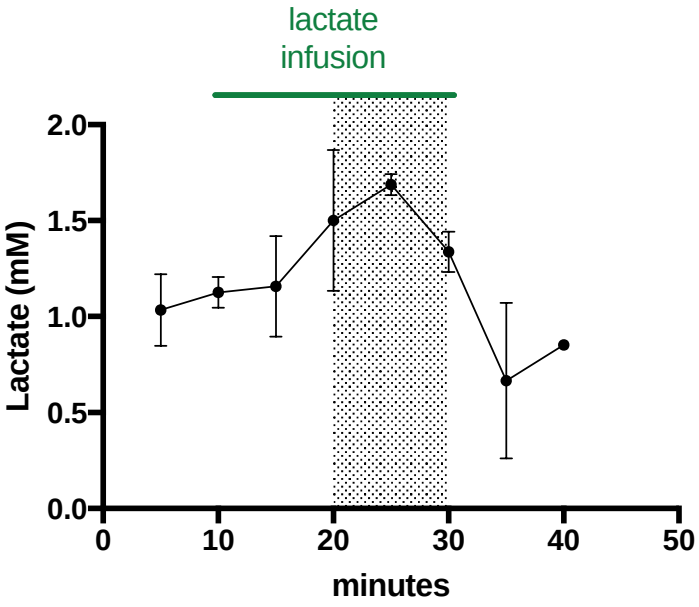

Supplementary Figure 1

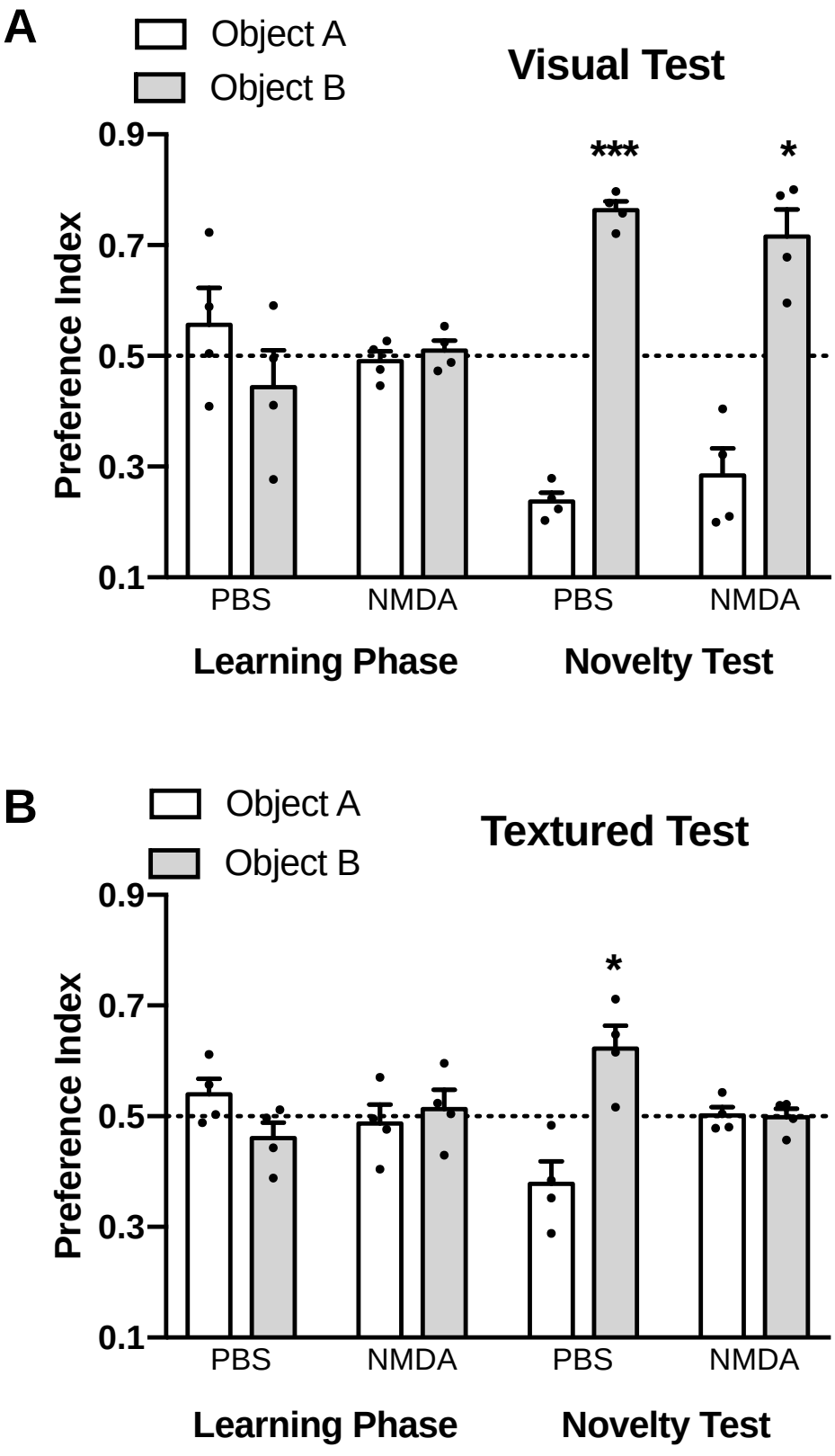

Supplementary Figure 2

	Ctr		MCT2		MCT4	
	S1BF -	S1BF +	S1BF -	S1BF +	S1BF -	S1BF +
Lac C3	8.62 ± 0.70	11.28 ± 0.58*	10.69 ± 0.72	10.98 ± 0.85	10.42 ± 0.85	10.17 ± 0.91
Ala C3	12.49 ± 0.75	13.97 ± 0.95	13.62 ± 0.61	13.93 ± 1.10	13.04 ± 0.70	13.29 ± 0.72
GABA C2	13.33 ± 0.70	13.78 ± 0.86	13.49 ± 0.67	14.37 ± 1.20	13.84 ± 0.75	12.84 ± 0.46
Glu C4	13.23 ± 1.13	12.95 ± 1.11	14.33 ± 0.87	13.16 ± 1.54	12.38 ± 0.99	13.43 ± 0.85
Gln C4	11.08 ± 1.18	7.33 ± 1.15*	7.61 ± 1.22	8.57 ± 1.49	8.85 ± 1.57	10.29 ± 1.09
Asp C3	9.71 ± 1.09	11.72 ± 1.27	10.23 ± 0.98	12.06 ± 0.89	9.11 ± 0.80	10.29 ± 0.89

Supplementary Table 1